Supplementary Information

Actomyosin bundles serve as a tension sensor and a platform for ERK activation

Hiroaki Hirata, Mukund Gupta, Sri Ram Krishna Vedula, Chwee Teck Lim, Benoit Ladoux and Masahiro Sokabe

Appendix

When tips of a stress fiber (SF) are anchored to the extracellular substratum through focal adhesions, uniaxial stretching of the substratum causes strain in the SF. As discussed below, the strain along the length of a SF should depend on orientation of the SF with respect to the stretch axis.

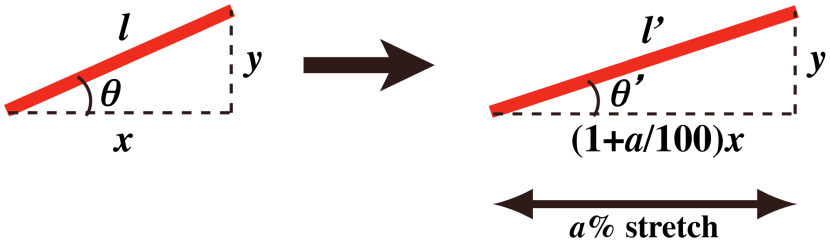

As shown in the above drawing, we assume that a SF (red line) is tilted with an angle θ with respect to the stretch axis, and the SF length is changed from l to l' upon uniaxial stretching. An a% stretch extends the parallel component of SF from x to $(1+a/100)x$, whereas the perpendicular component (y) remains unchanged. Resultant strain along the length of a SF can then be expressed as

$$S \equiv \frac{l'}{l} - 1 = \frac{\sqrt{(1+a/100)^2 x^2 + y^2}}{\sqrt{x^2 + y^2}} - 1. \qquad [1']$$

Since y is expressed as $x \times \tan\theta$, the equation [1'] is re-expressed as

$$S = \sqrt{\frac{(1+a/100)^2 + \tan^2\theta}{1+\tan^2\theta}} - 1 = \sqrt{(1+a/100)^2 \cos^2\theta + \sin^2\theta} - 1, \qquad [2']$$

which shows dependency of the SF strain on the SF angle against the stretch axis.

The SF angle changes upon stretching (from θ to θ' in the above drawing). For microscopic observation of stretched cells, the elastic chamber was removed from the stretching device and mounted onto the microscope stage. Hence, we observed cells and

measured the SF angle under the condition where stretch-induced strain was released. Therefore, we used the initial angle θ, not the angle θ' under the stretched condition, as the SF angle in this study.

Supplementary Methods

Antibodies and chemicals

Mouse and rabbit monoclonal antibodies (mAbs) against phosphorylated ERK 1/2, and the rabbit polyclonal antibody (pAb) against ERK 1/2 were purchased from Cell Signaling Technology (Danvers, MA). For immunofluorescence staining of phosphorylated ERK, the mouse mAb against phosphorylated ERK 1/2 was used unless otherwise indicated. The rabbit anti-Ser380-phosphorylated RSK and anti-RSK1/RSK2/RSK3 mAbs were from Cell Signaling Technology. The mouse anti-E-cadherin mAb was from Becton, Dickinson and Company (Franklin Lakes, NJ). The mouse anti-β-actin mAb was from Sigma Chemical. Alexa Fluore 488-goat anti-mouse IgG, Alexa Fluore 488-goat anti-rabbit IgG and Alexa Fluore 546-goat anti-mouse IgG antibodies, and Alexa Fluore 546- and Alexa Fluore 647-phalloidin were from Life Technologies. Horseradish peroxidase-conjugated anti-mouse IgG and anti-rabbit IgG antibodies were from GE Healthcare (Little Chalfont, UK). Hoechst 33258, cytochalasin D, CGP7675 and DMSO were from Sigma Chemical. Blebbistatin and focal adhesion kinase inhibitor II were from Toronto Research Chemicals (North York, Canada) and Merck Millipore (Billerica, MA), respectively.

Immunofluorescence

Cells were fixed and permeabilized for 30 min with 4% formaldehyde and 0.2% Triton X-100 in cytoskeleton stabilizing buffer (137 mM NaCl, 5 mM KCl, 1.1 mM Na_2HPO_4, 0.4 mM KH_2PO_4, 4 mM $NaHCO_3$, 2 mM $MgCl_2$, 5.5 mM glucose, 2 mM EGTA, and 5 mM PIPES, pH 6.1). This was followed by blocking with 1% BSA in cytoskeleton stabilizing buffer for 30 min. The cells were then incubated with primary antibodies for 40 min, washed, and further incubated with secondary antibodies (and fluorescent phalloidin, when necessary) for 40 min. Antibodies were diluted to 1:100 in cytoskeleton stabilizing buffer containing 1% BSA.

The cells were observed with an epi-fluorescence inverted microscope (IX81, OLYMPUS, Tokyo, Japan) equipped with an oil immersion (NA 1.45, 100×; PlanApo, OLYMPUS) or a water immersion (NA 1.20, 60×; UPlanSApo, OLYMPUS) objective and a charge-coupled device camera (CoolSNAP EZ, Photometrics, Tucson, AZ). The Metamorph software (Molecular Devices, Sunnyvale, CA) was used for image acquisition. The bleed-through effect of fluorescence signals through different fluorescence channels was negligible (Fig. S17). A confocal microscope (TCS SP5, Leica Microsystems, Wetzlar, Germany) equipped with an oil immersion objective (NA 1.40, 100×; HCX PL APO CS, Leica Microsystems) was also used (Fig. S1). Acquired images were analyzed offline using the public domain software ImageJ (version 1.45f).

Integrated intensities of F-actin on SFs in their width direction were measured as follows. The fluorescence intensity profile of F-actin ($I(x)$) in the width direction of an SF was fitted with the Gaussian function,

$$I(x) = a + b\exp\left(-\frac{(x-c)^2}{2d^2}\right), \qquad [3']$$

where a, b, c and d are fitting parameters, and a represents the basal level of the fluorescence intensity (Fig. S18). The integrated intensity of F-actin (M) was then calculated, as

$$M = \int_{-\infty}^{\infty} b\exp\left(-\frac{(x-c)^2}{2d^2}\right)dx = \sqrt{2\pi}bd \quad , \qquad [4']$$

which reflects the amount of F-actin in the SF in its width direction (Fig. S18).

Plasmids and shRNA-mediated depletion of ERK expression

Plasmids for expression of EGFP-vinculin and α-actinin-mCherry were gifted from Dr. Cheng-Han Yu (National University of Singapore) and Dr. Hiroaki Machiyama (National University of Singapore), respectively. F-actin in living cells was visualized by expressing F-Tractin-tdTomato [53]. Expression of ERK proteins in HFFs was depleted by retrovirus-mediated introduction of shRNA into cells, as described previously [49]. The target sequences used were 5′-GCCATGAGAGATGTCTACA-3′ (for ERK1) and 5′-GTTCGAGTAGCTATCAAGA-3′ (for ERK2). As a control, shRNA with the non-targeting sequence (5′-ATAGTCACAGACATTAGGT-3′) was used. These sequences were inserted into the pSUPER.puro vector.

Stretching-cell assay

Stretching-cell assays were performed as described previously [17]. In brief, HFFs or NIH3T3 cells grown on elastic silicone chambers were first treated with 100 μM blebbistatin for 30 min, and then uniaxially stretched by 50% for 5 min in the presence of blebbistatin. A home-made manual stretching device was used for immunofluorescence and immunoblotting experiments. For live cell imaging, a pulse-motor-driven stretching device (ST-600W, Strex) was mounted onto an upright microscope (Axio Imager Z2m, Carl Zeiss, Oberkochen, Germany) equipped with a water immersion (NA 0.9, 63×; W N-Achroplan, Carl Zeiss) objective and an electron-multiplying charge-coupled device camera (Cascade II:1024, Photometrics).

Force measurement using μFSA

Microforce sensor arrays (μFSA) comprising of pillars (diameter, 2 μm; height, 7 μm; center-to-center distance, 4 μm) were prepared as described previously [43]. Briefly, PDMS (1/10 cross-linker to base polymer ratio) was poured on silicone molds and cured at 80°C for 2 h to obtain Young's modulus of 2 MPa. The resulting stiffness of the substrate used was 43 nN/μm. The tops of the micropillars were selectively coated with dye-conjugated fibronectin using the micro-contact printing technique, and their sides were made non-adhesive by treating with 0.2% Pluronics-F127. A home-made plugin developed for ImageJ was used to detect the centroids of deflected micropillars, calculate the force field for the substrate and visualize it in form of vectors. Pillars with multiple SF connections were excluded from analyses (Fig. S19A). Since some SFs showed branching in the middle (Fig. S19B), we used the SF regions only within 5 μm from their tips for analyses of pERK intensities (Fig. S19C).

Immunoblot

Cells were lysed with 2× lithium dodecyl sulfate sample buffer (Life Technologies) containing 2.5% β-mercaptoethanol. The lysate samples were resolved by SDS-PAGE (4-12% Bis-Tris gel; Life Technologies), transferred onto a polyvinylidene fluoride membrane (Merck Millipore), and probed with antibodies. Immuno-reactive bands were detected with SuperSignal West Pico Chemiluminescent Substrate (Thermo Fisher

Scientific, Rockford, IL).

Statistical analysis

Bar graphs were presented as means ± SD. Statistical significance was assessed using Student's two-tailed, unpaired *t*-test.

Supplementary References

[53] Johnson HW, Schell MJ (2009) Neuronal IP_3 3-kinase is an F-actin-bundling protein: role in dendritic targeting and regulation of spine morphology. *Mol Biol Cell* **20:** 5166-5180

Supplementary Figure Legends

Fig. S1. Confocal observations of localization of pERK and ERK on SFs. (A) A HFF double-stained for pERK and F-actin was observed with confocal microscopy. Upper panels: z-projection images. Lower panels: z-section images along the white line in the upper left panel. Merged images are also shown. Horizontal bars, 40 μm; vertical bar, 5 μm. (B and C) Confocal images of HFFs treated with either DMSO or 100 μM blebbistatin (Blebb) for 30 min, and then double-stained for F-actin and either pERK (B) or total ERK (C). Merged images are also shown. Bars, 40 μm. (D) Quantification results of pERK (black bar) and ERK (gray bar) intensities on individual SFs in HFFs treated with either DMSO or 100 μM blebbistatin (Blebb). Sample values were normalized with respect to the mean values of control (DMSO) samples. 42 SFs in 7 cells (pERK, DMSO), 36 SFs in 9 cells (pERK, Blebb), 38 SFs in 10 cells (ERK, DMSO) and 29 SFs in 13 cells (ERK, Blebb) were analyzed.

Fig. S2. Myosin II-dependent localization of pERK to the actin cytoskeleton in NIH3T3 cells. NIH3T3 cells treated with either DMSO or 100 μM blebbistatin (Blebb) for 30 min were double-stained for pERK and F-actin. Merged images are also shown. There was little accumulation of pERK at cortical F-actin in blebbistatin-treated NIH3T3 cells

(arrows). Bar, 20 μm.

Fig. S3. Localized staining of pERK on SFs was obtained with different antibodies against phosphorylated ERK. (A) Immunoblot characterization of antibodies. Lysates from HFFs were probed with the mouse (Ms) or the rabbit (Rb) mAb against phosphorylated ERK or with rabbit pAb against ERK. (B) HFFs were double-stained for F-actin and pERK using either the mouse (Ms) or the rabbit (Rb) anti-phosphorylated ERK mAb. Both mAbs gave localized staining on SFs (arrows). Bar, 40 μm.

Fig. S4. Exclusion of pERK distribution from α-actinin-rich puncta on SFs and from FAs. (A) HFFs expressing α-actinin-mCherry were stained for pERK. The merged image is also shown. (B) Fluorescence intensity profiles of pERK (green) and α-actinin-mCherry (red) along a single SF. Intensity values were normalized with respect to the maximum value in each profile. (C) HFFs expressing EGFP-vinculin as a FA marker were stained for pERK. The merged image is also shown. Bars, 10 μm for (A) and 20 μm for (C).

Fig. S5. Effect of shRNA-mediated depletion of ERK expression on immunostaining of pERK and ERK. (A) HFFs expressing non-targeting shRNA (shContl) or shRNA against ERK1 (shERK1) or ERK2 (shERK2) were lysed and immunoblotted for pERK, ERK and β-actin. (B) HFFs expressing non-targeting shRNA (shContl) or shRNA against ERK1 (shERK1) or ERK2 (shERK2) were double-stained for F-actin and either pERK (upper 6 panels) or total ERK (lower 6 panels). Bar, 40 μm.

Fig. S6. Residual SFs in blebbistatin-treated HFFs. (A) HFFs treated with either DMSO or 100 μM blebbistatin (Blebb) for 30 min were stained for F-actin. Bar, 40 μm. (B) Fluorescence intensity profiles of F-actin along yellow lines in (A). Consistently with previous reports [17,18], residual SFs were observed in HFFs treated with 100 μM blebbistatin for 30 min. However, the number of SFs and the fluorescence intensity of F-actin on SFs were highly decreased upon the blebbistatin treatment.

Fig. S7. Immunoblotting analyses of effects of myosin II inhibition and mechanical

stretching on ERK phosphorylation. (A) NIH3T3 cells cultured on FN-coated elastic substrata were treated with either DMSO or 100 μM blebbistatin (Blebb) for 30 min, and then the substrata were uniaxially stretched (50% for 5 min) in the presence of blebbistatin, when indicated. The cells were analyzed by immunoblotting for pERK and total ERK. The bar graph shows quantification of the densitometric ratio of pERK against ERK (N = 3). Sample values were normalized with respect to the mean value of control (- Blebb, - stretch) samples. (B) NIH3T3 cells cultured on FN-coated elastic substrata were subjected to uniaxial stretching (50% for 5 min) when indicated, and were analyzed by immunoblotting for pERK and total ERK.

Fig. S8. Myosin II-dependent nuclear localization of pERK. (A) HFFs treated with either DMSO or 100 μM blebbistatin (Blebb) for 30 min were double-stained for pERK and nuclei (with Hoechst). Bar, 40 μm. (B) Fluorescence intensity profiles of pERK (green) and Hoechst (blue) along white lines across nuclei in (A).

Fig. S9. Live observations of stretch-induced reinforcement of F-actin bundles. (A) HFFs expressing F-Tractin-tdTomato were cultured on FN-coated elastic substrata, treated with 100 μM blebbistatin for 30 min, and then subjected to sustained uniaxial stretching in the presence of blebbistatin under microscopic observations. Images before and after stretching for 5min are shown. Double-headed arrows indicate the direction of stretching. In cells oriented at small angles against the stretch axis, reinforcement of F-actin bundles was observed after stretching (yellow arrows). (B) Magnified images of outlined regions in (A). Merged images are also shown. Bars, 50 μm for (A) and 10 μm for (B).

Fig. S10. The relationship between the F-actin amount in individual SFs in their width direction and SF strain induced by 50% stretch. The intensities were normalized with respect to the maximum value. Strain in SFs was calculated from the SF angles using the equation [1]. The blue line represents the linear fitting. C.C., correlation coefficient.

Fig. S11. Tensile force-dependent ERK phosphorylation on SFs in a single myosin II-inhibited cell upon mechanical stretching. (A) A HFF cultured on FN-coated elastic substratum was treated with 100 μM blebbistatin for 30 min, and then the substratum

was uniaxially stretched (50% for 5 min) in the presence of blebbistatin (Blebb + stretch). The cell was double-stained for pERK and F-actin. The merged image is also shown. Double-headed arrows indicate the direction of stretching. Bar, 40 μm. (B) The averaged intensities of pERK along individual SFs in the cell shown in (A) were plotted against the SF angles. The intensities were normalized with respect to the maximum value. The blue line represents the linear fitting. C.C., correlation coefficient. (C) For the same data set as that in (B), the averaged intensities of pERK along individual SFs were re-plotted against relative tensile forces in the SFs. Relative tensile forces in SFs were calculated from the SF angles using the equation [1] and the regression equation in Fig. 2D. The intensities were normalized with respect to the maximum value. The blue line represents the linear fitting. C.C., correlation coefficient.

Fig. S12. Disruption of the actin cytoskeleton abrogated stretch-induced ERK phosphorylation. (A) NIH3T3 cells cultured on FN-coated elastic substrata were treated with 100 μM blebbistatin (Blebb) and either DMSO or 10 μM cytochalasin D (CytoD) for 30 min, and then the substrata were uniaxially stretched (50% for 5 min) in the presence of blebbistatin and either DMSO or cytochalasin D, when indicated. The cells were analyzed by immunoblotting for pERK, total ERK, Ser379 (Ser380 in human RSK1)-phosphorylated RSK and total RSK. (B) HFFs cultured on FN-coated elastic substrata were treated with 100 μM blebbistatin (Blebb) and either DMSO or 10 μM cytochalasin D (CytoD) for 30 min, and the substrata were uniaxially stretched (50% for 5 min) in the presence of blebbistatin and either DMSO or cytochalasin D, when indicated. The cells were then double-stained for pERK and F-actin. Double-headed arrows indicate the direction of stretching. Bar, 40 μm.

Fig. S13. Actomyosin bundles in suspended epithelial bridges connect between E-cadherin clusters. Epithelial bridges of HaCaT cells formed over non-adhesive regions were stained for E-cadherin (E-Cad), F-actin and nuclei. The magnified and merged image of E-cadherin (E-Cad) and F-actin in the outlined region is also shown. Bars, 40 μm for upper 4 panels, and 20 μm for the magnified image.

Fig. S14. Epithelial bridges of HaCaT cells formed over non-adhesive regions were double-stained for F-actin and pERK. The merged image of pERK and F-actin is also

shown. pERK was localized on actomyosin bundles in suspended epithelial bridges (arrows), but not at F-actin accumulations at cell-cell boundaries in the FN region (double-arrowheads). Bar, 40 μm.

Fig. S15. Involvement of Src and FAK in ERK phosphorylation. HFFs were treated with either DMSO, 10 μM CGP77675 (Src inhibitor) or 10 μM focal adhesion kinase inhibitor II (FAK inhibitor) for 30 min. The cells were then analyzed by immunoblotting for pERK and total ERK (A) and by immunostaining for pERK and F-actin (B). Bar, 40 μm.

Fig. S16. Serum starvation abrogated stretch-induced ERK phosphorylation. (A and B) HFFs without (control) and with (starved) serum starvation for 3 days were double-stained for F-actin and either pERK (A) or total ERK (B). Arrows denote ERK localization on F-actin bundles in serum-starved cells. Bars, 40 μm. (C) HFFs cultured on FN-coated elastic substrata were subjected to serum starvation for 3 days, and the substrata were uniaxially stretched (50% for 5 min) in the absence of serum, when indicated. The cells were then double-stained for pERK and F-actin. Double-headed arrows indicate the direction of stretching. Bar, 40 μm. (D) NIH3T3 cells cultured on FN-coated elastic substrata were subjected to serum starvation for 3 days, and the substrata were uniaxially stretched (50% for 5 min) in the absence of serum, when indicated. The cells were then analyzed by immunoblotting for pERK and total ERK.

Fig. S17. The bleed-through effect of fluorescence signals through different fluorescence channels was negligible. HFFs were stained with fluorescently labeled phalloidin and/or either the anti-pERK (A) or anti-ERK (B) antibody. Bars, 40 μm.

Fig. S18. Calculation of the integrated intensity of F-actin on an SF in its width direction. (A) An image of F-actin staining. (B) Fluorescence intensities along the line across an SF (yellow line in A) were plotted, and the plots were fitted with the Gaussian function (blue line). The area *M* surrounded by the Gaussian curve (blue line) and the base line (red line) represents the integrated intensity of F-actin, which reflects the amount of F-actin in the SF in its width direction.

Fig. S19. Criteria of choosing pillars and SFs used for analyses. Red; fluorescent FN-coated pillar tips, green; F-actin. (A) Some SFs have branching (arrows) in their middle portion. (B) The SF regions within 5 μm from their tips were used for analyzing intensities of phosphorylated ERK on SFs. (C) Pillars with multiple SF connections (arrow) were excluded from analyses.

Movie 1. Live observations of stretch-induced reinforcement of F-actin bundles. HFFs expressing F-Tractin-tdTomato were cultured on FN-coated elastic substrata, treated with 100 μM blebbistatin for 30 min, and then subjected to sustained uniaxial stretching in the presence of blebbistatin under microscopic observations. Images acquired before and after stretching for 5min are shown at the speed of 1 frame per second. Two cells with different orientation angles against the stretch axis are shown.

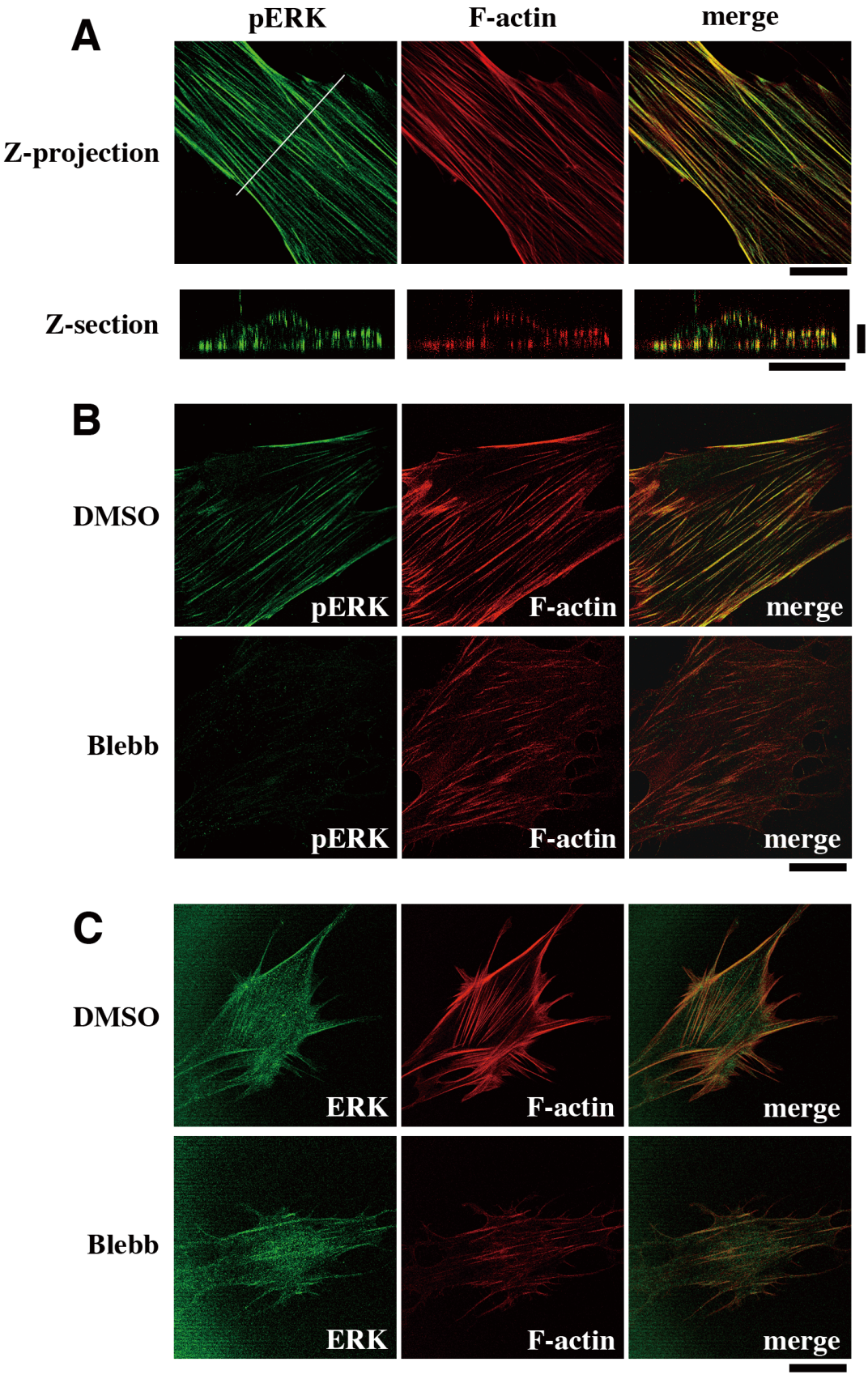
A
pERK
F-actin
merge
Z-projection
Z-section
B
DMSO
pERK
F-actin
merge
Blebb
pERK
F-actin
merge
C
DMSO
ERK
F-actin
merge
Blebb
ERK
F-actin
merge
D
p < 0.01
p < 0.01
pERK/F-actin ■
or
ERK/F-actin □
1.5
1
0.5
0
DMSO
Blebb

Fig. S1

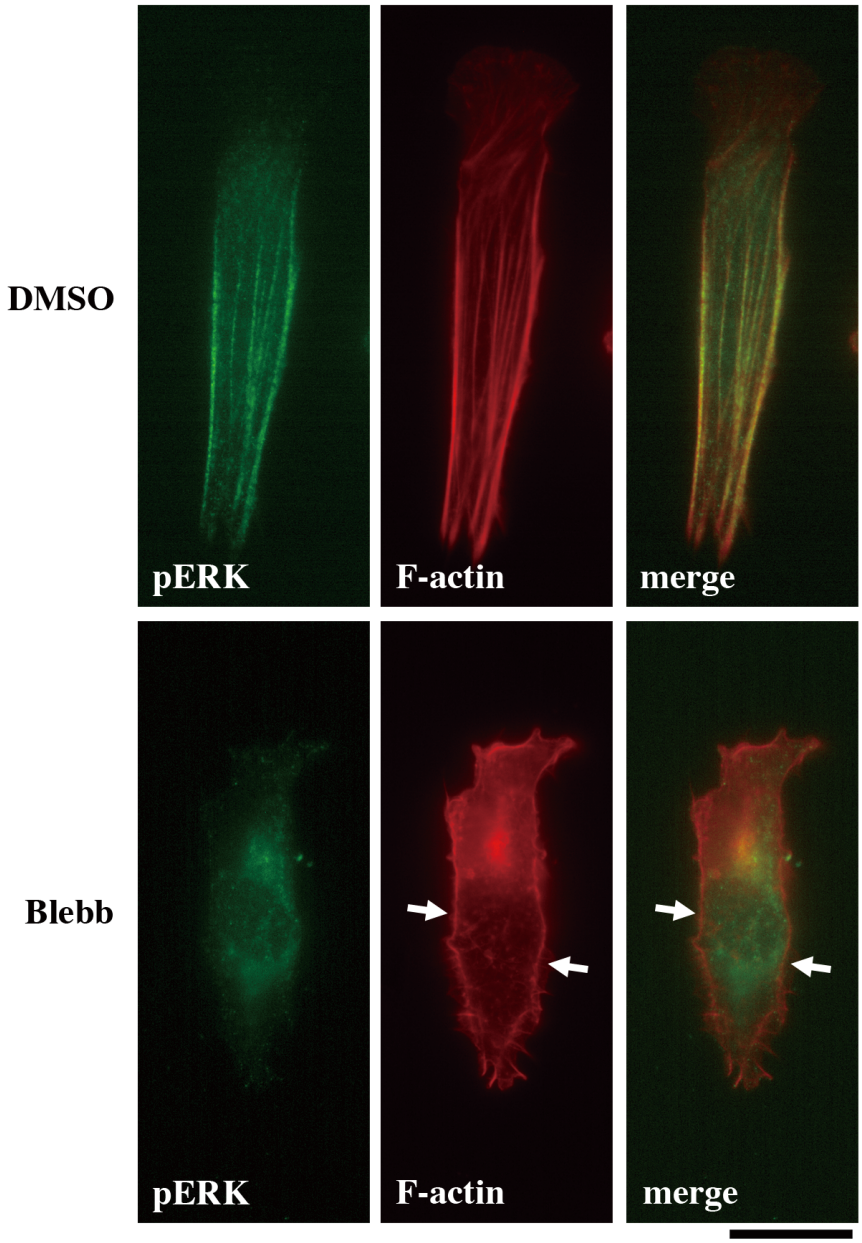

Fig. S2

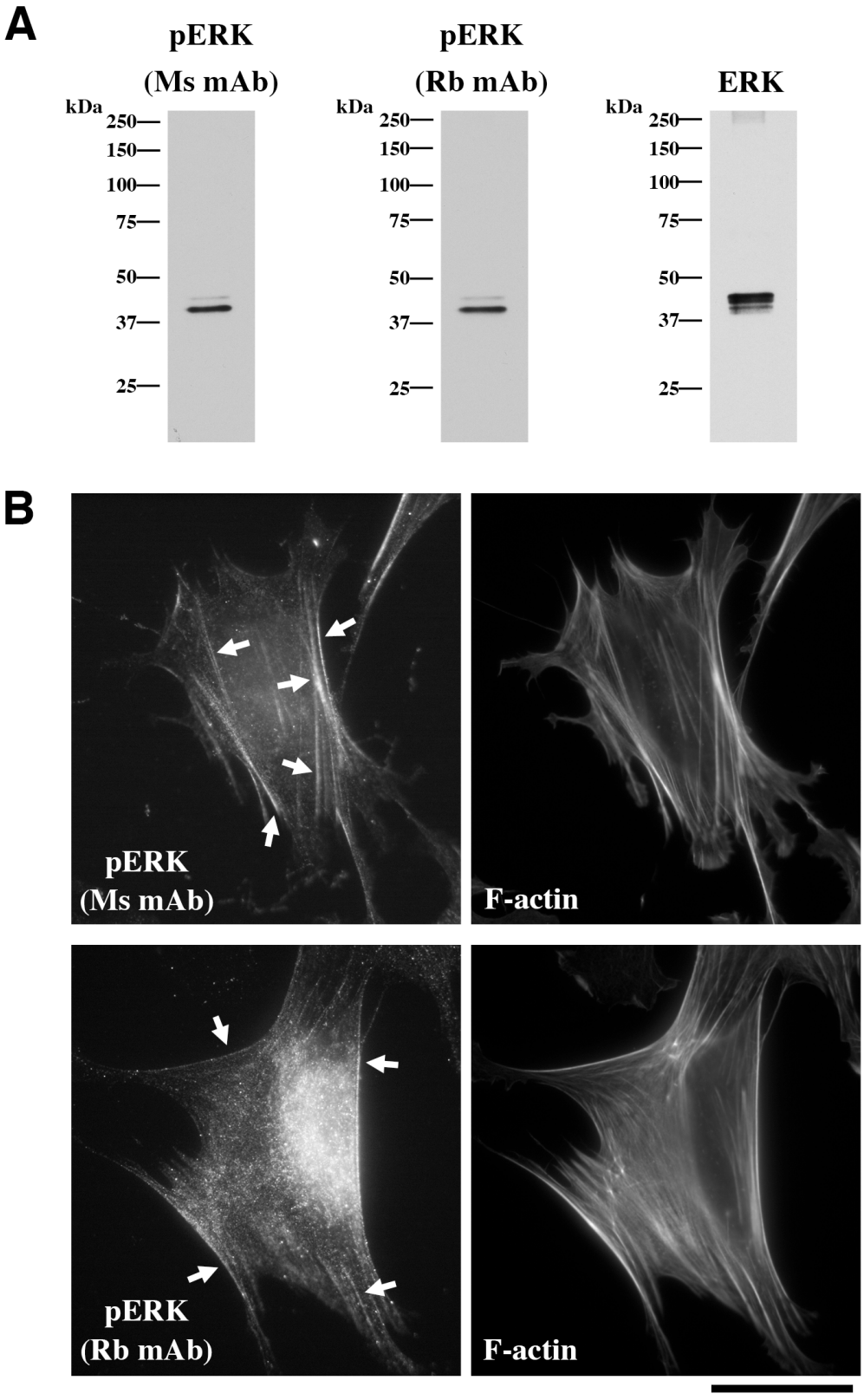
A
pERK
(Ms mAb)
pERK
(Rb mAb)
ERK
kDa
250
150
100
75
50
37
25
B
pERK
(Ms mAb)
F-actin
pERK
(Rb mAb)
F-actin

Fig. S3

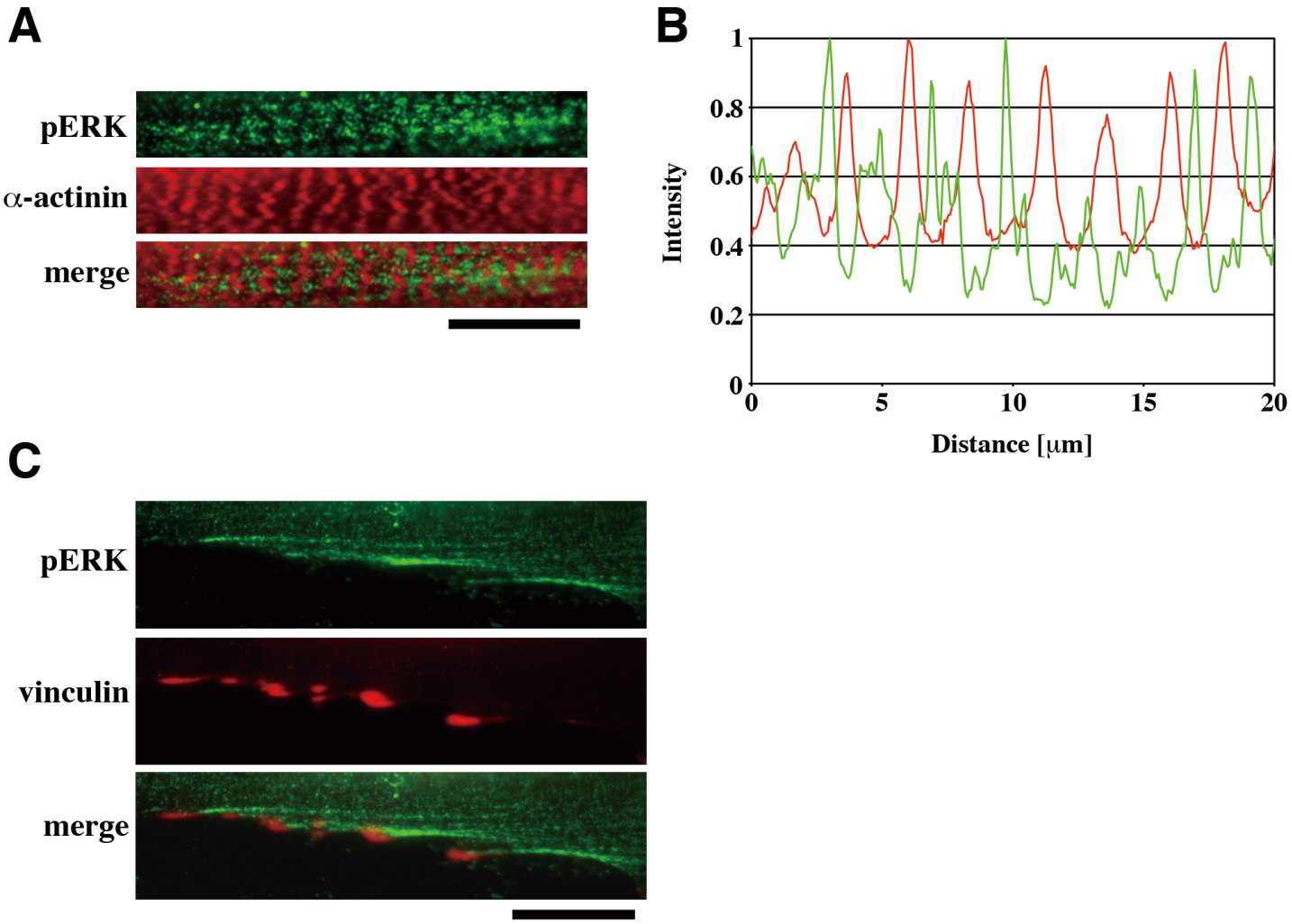
A
pERK
α-actinin
merge
B
Intensity
1
0.8
0.6
0.4
0.2
0
0
5
10
15
20
Distance [μm]
C
pERK
vinculin
merge

Fig. S4

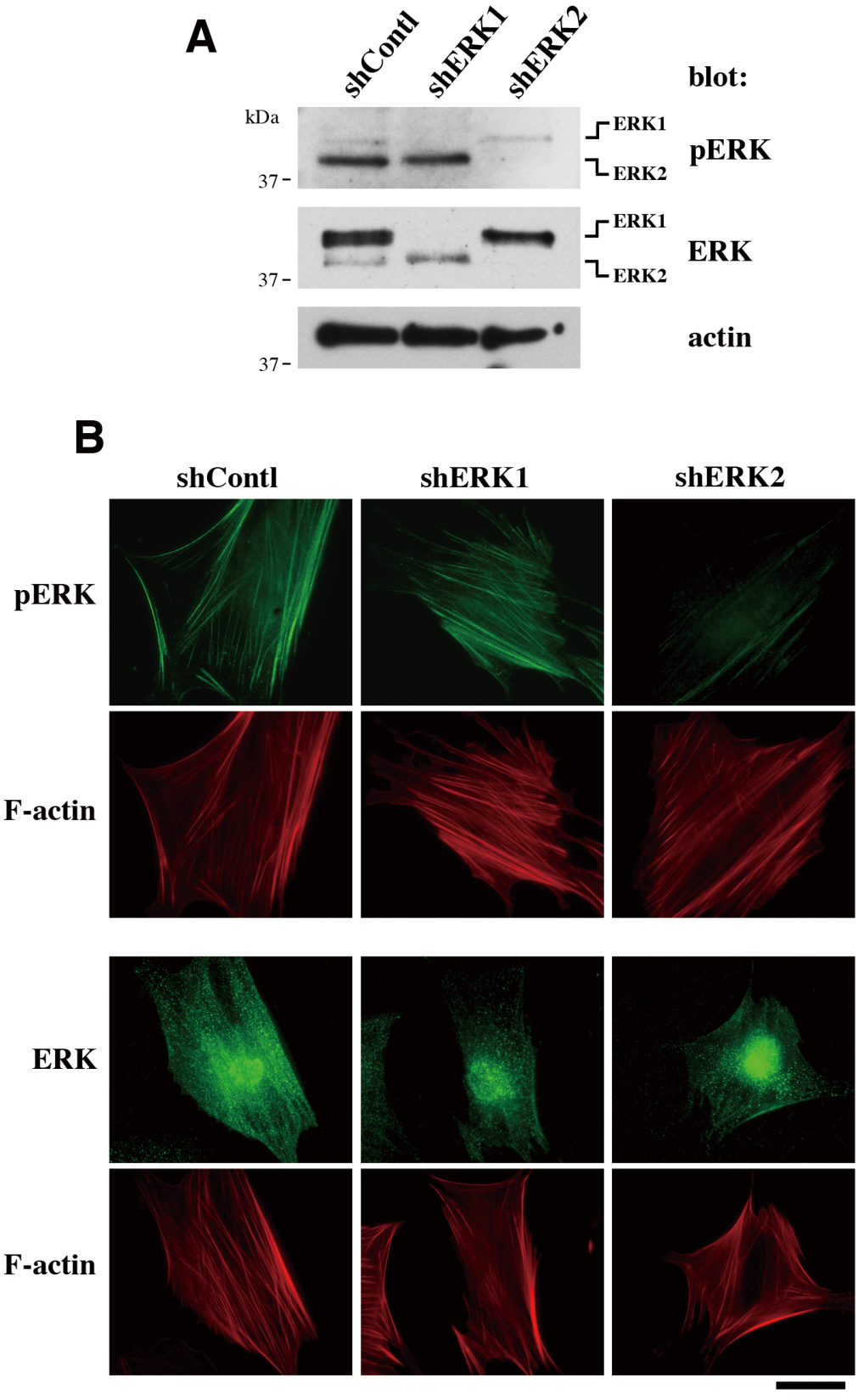
A
shContl
shERK1
shERK2
blot:
kDa
ERK1
ERK2
pERK
37
ERK1
ERK2
ERK
37
actin
37
B
shContl
shERK1
shERK2
pERK
F-actin
ERK
F-actin

Fig. S5

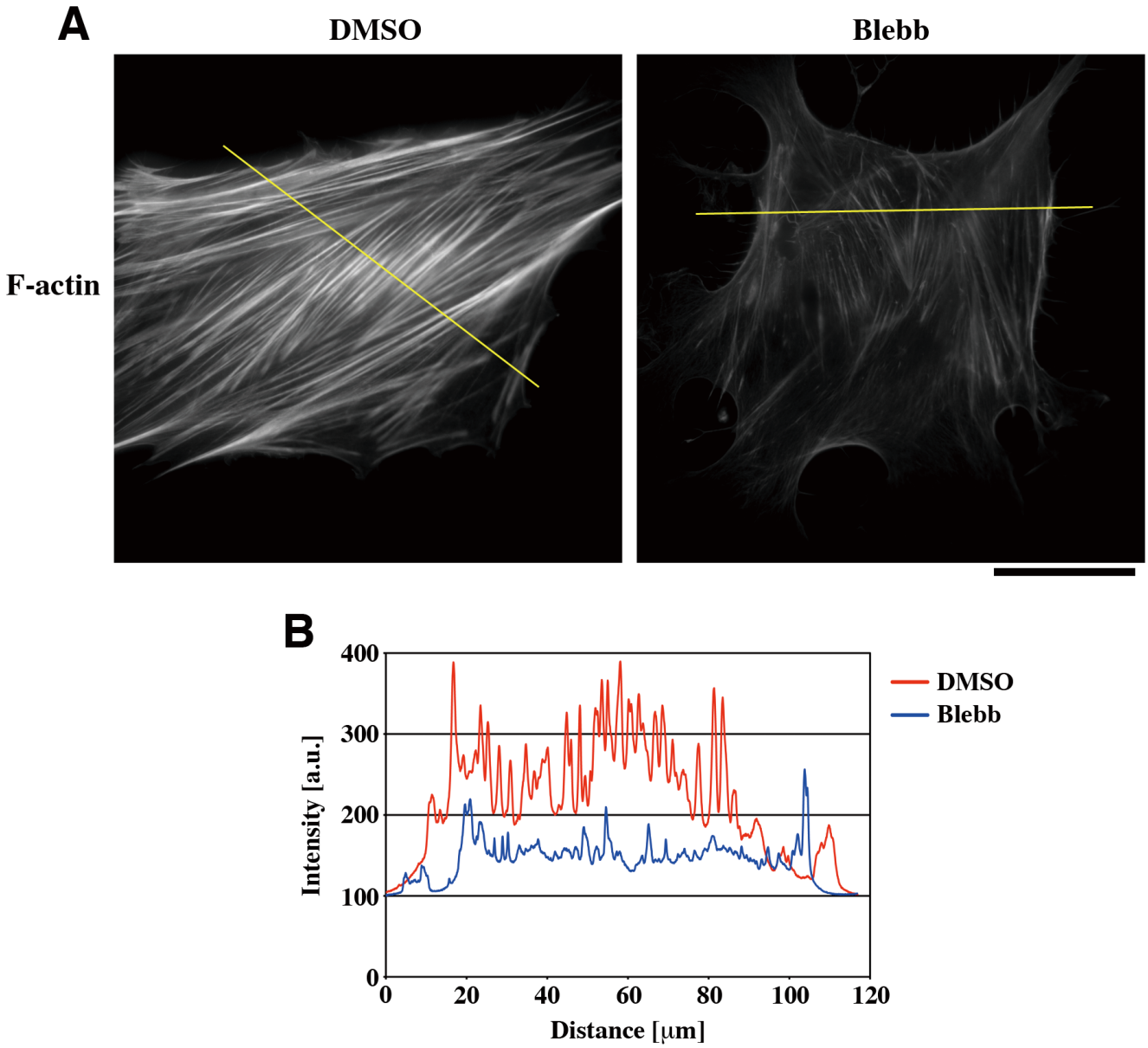
A
DMSO
Blebb
F-actin
B
400
300
200
100
0
Intensity [a.u.]
0
20
40
60
80
100
120
Distance [μm]
DMSO
Blebb

Fig. S6

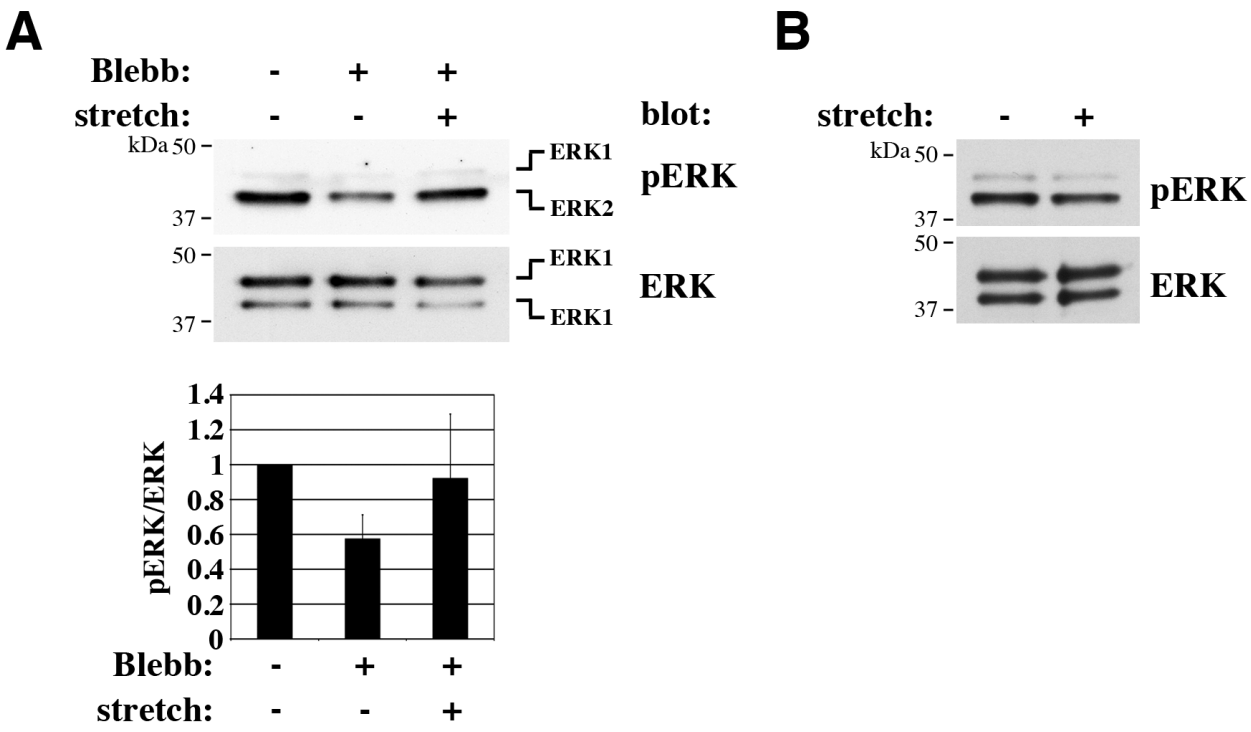
A
Blebb: - + +
stretch: - - +
kDa 50
37
ERK1
ERK2
50
37
ERK1
ERK1
blot:
pERK
ERK
1.4
1.2
1
0.8
0.6
0.4
0.2
0
pERK/ERK
Blebb: - + +
stretch: - - +
B
stretch: - +
kDa 50
37
pERK
50
37
ERK

Fig. S7

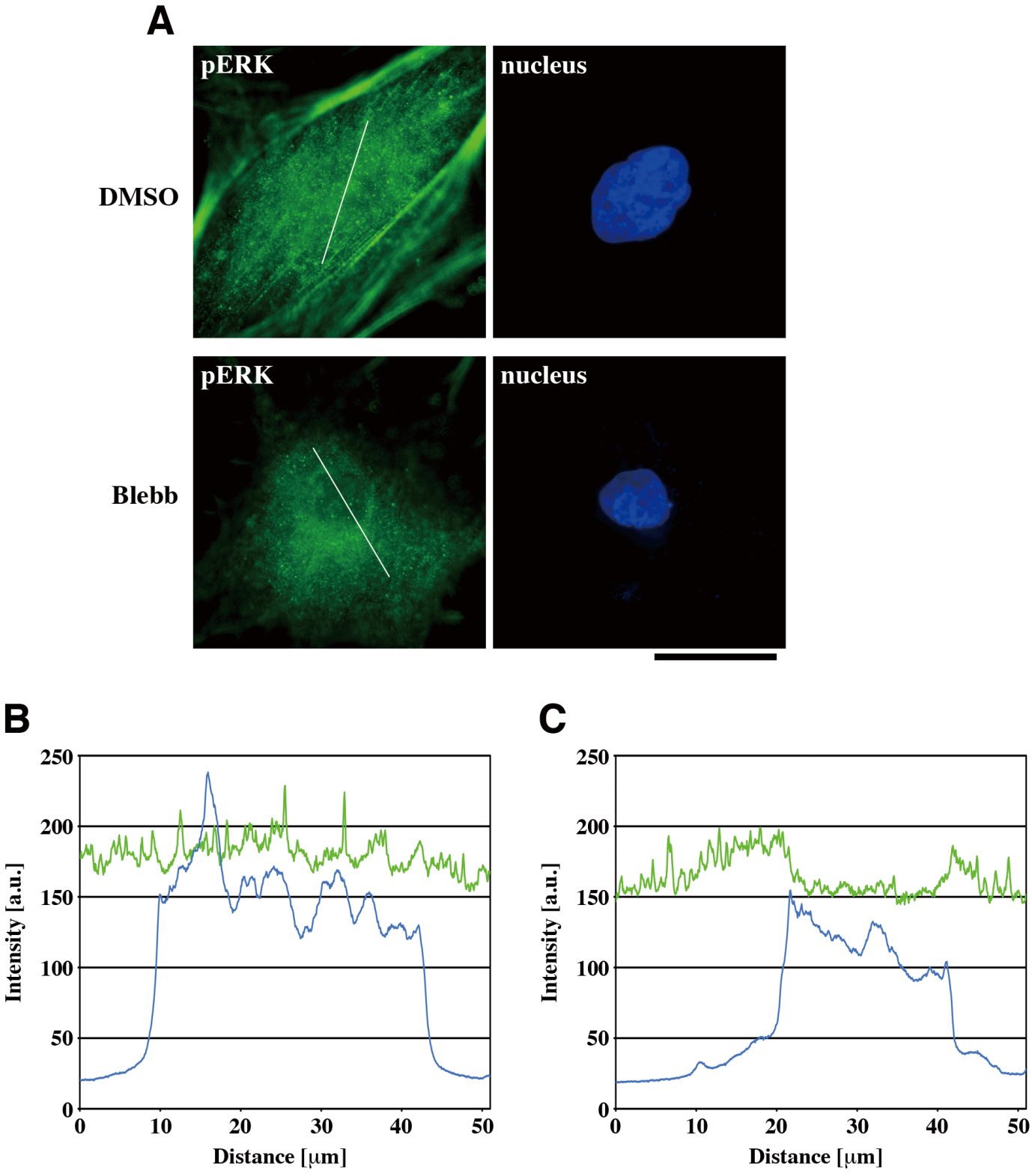
A
pERK
nucleus
DMSO
pERK
nucleus
Blebb
B
Intensity [a.u.]
250
200
150
100
50
0
0
10
20
30
40
50
Distance [μm]
C
Intensity [a.u.]
250
200
150
100
50
0
0
10
20
30
40
50
Distance [μm]

Fig. S8

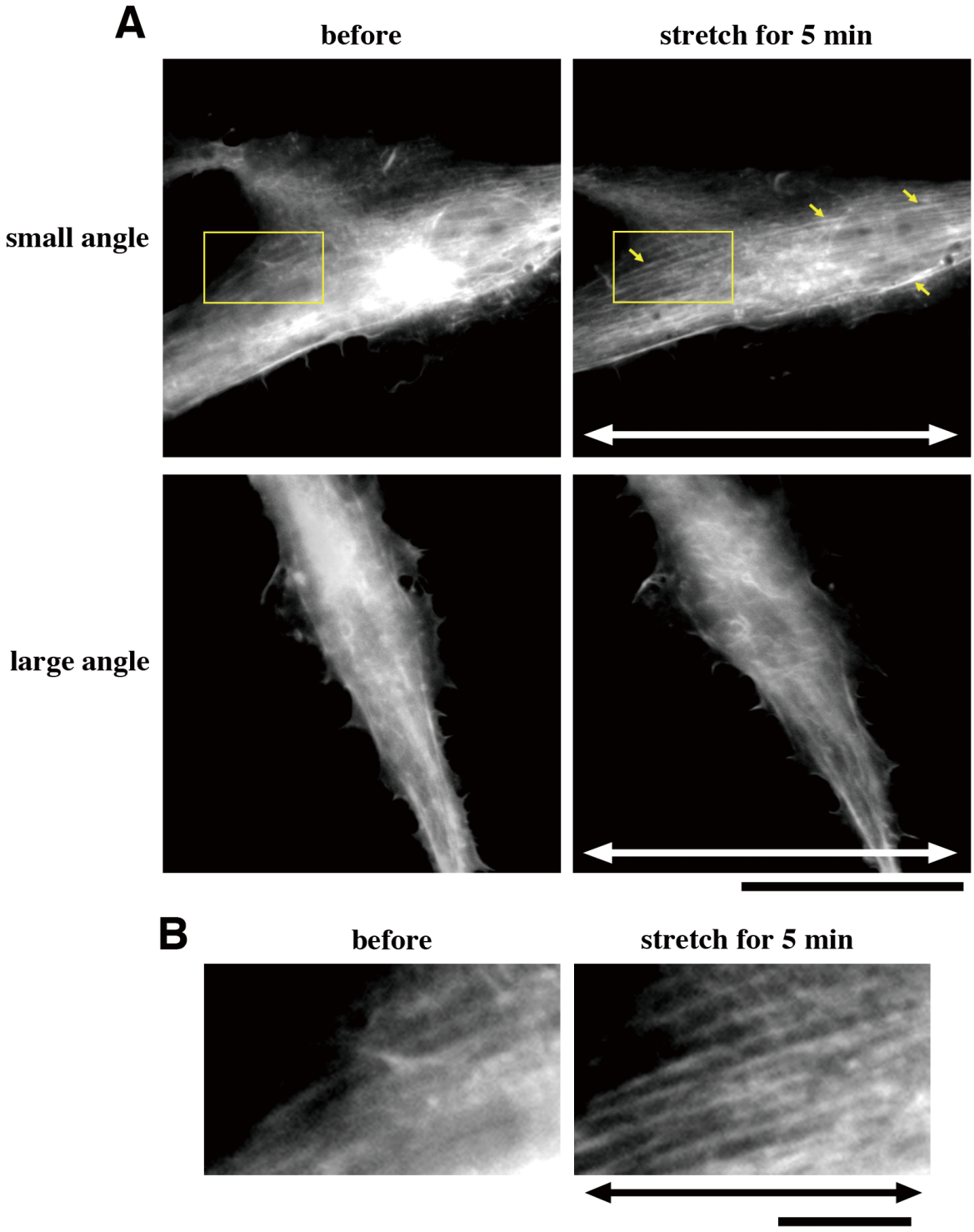
A
before
stretch for 5 min
small angle
large angle
B
before
stretch for 5 min

Fig. S9

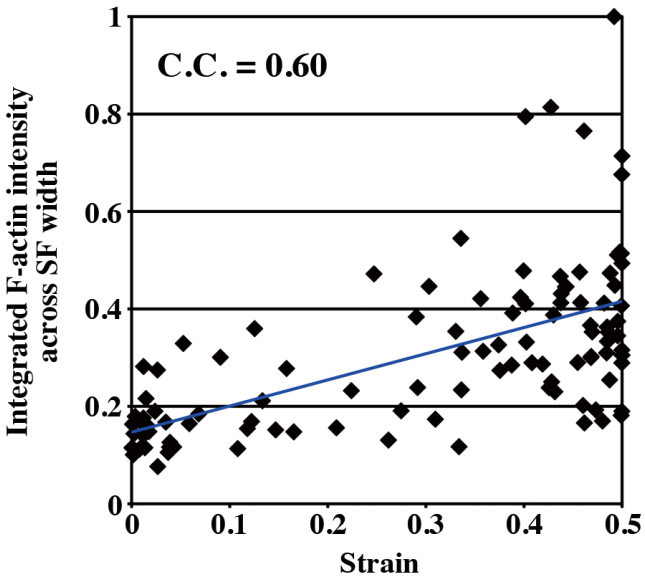
C.C. = 0.60
Integrated F-actin intensity across SF width
Strain
0
0.2
0.4
0.6
0.8
1
0
0.1
0.2
0.3
0.4
0.5

Fig. S10

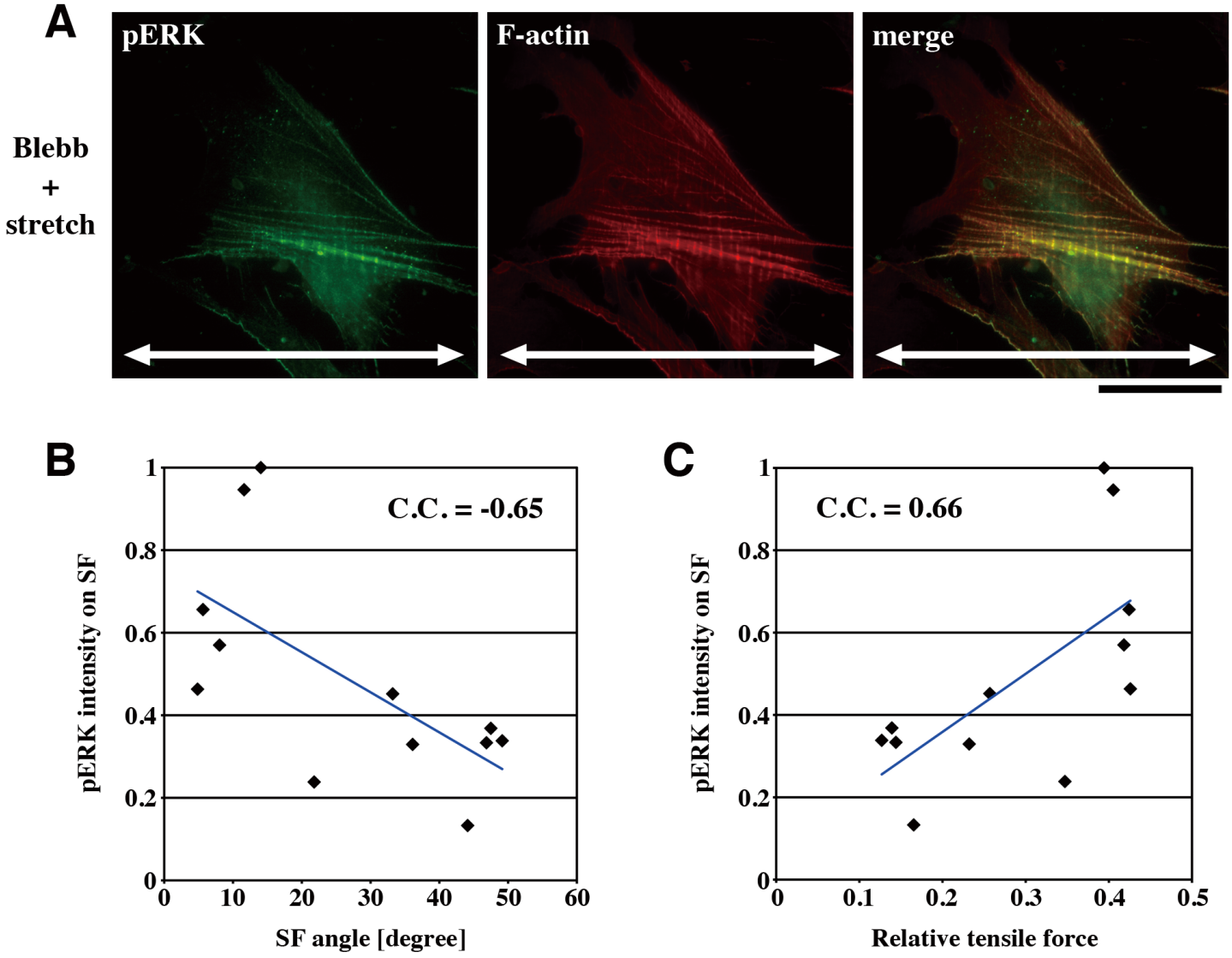
A
Blebb
+
stretch
pERK
F-actin
merge
B
C.C. = -0.65
pERK intensity on SF
SF angle [degree]
0
0.2
0.4
0.6
0.8
1
0
10
20
30
40
50
60
C
C.C. = 0.66
pERK intensity on SF
Relative tensile force
0
0.1
0.2
0.3
0.4
0.5

Fig. S11

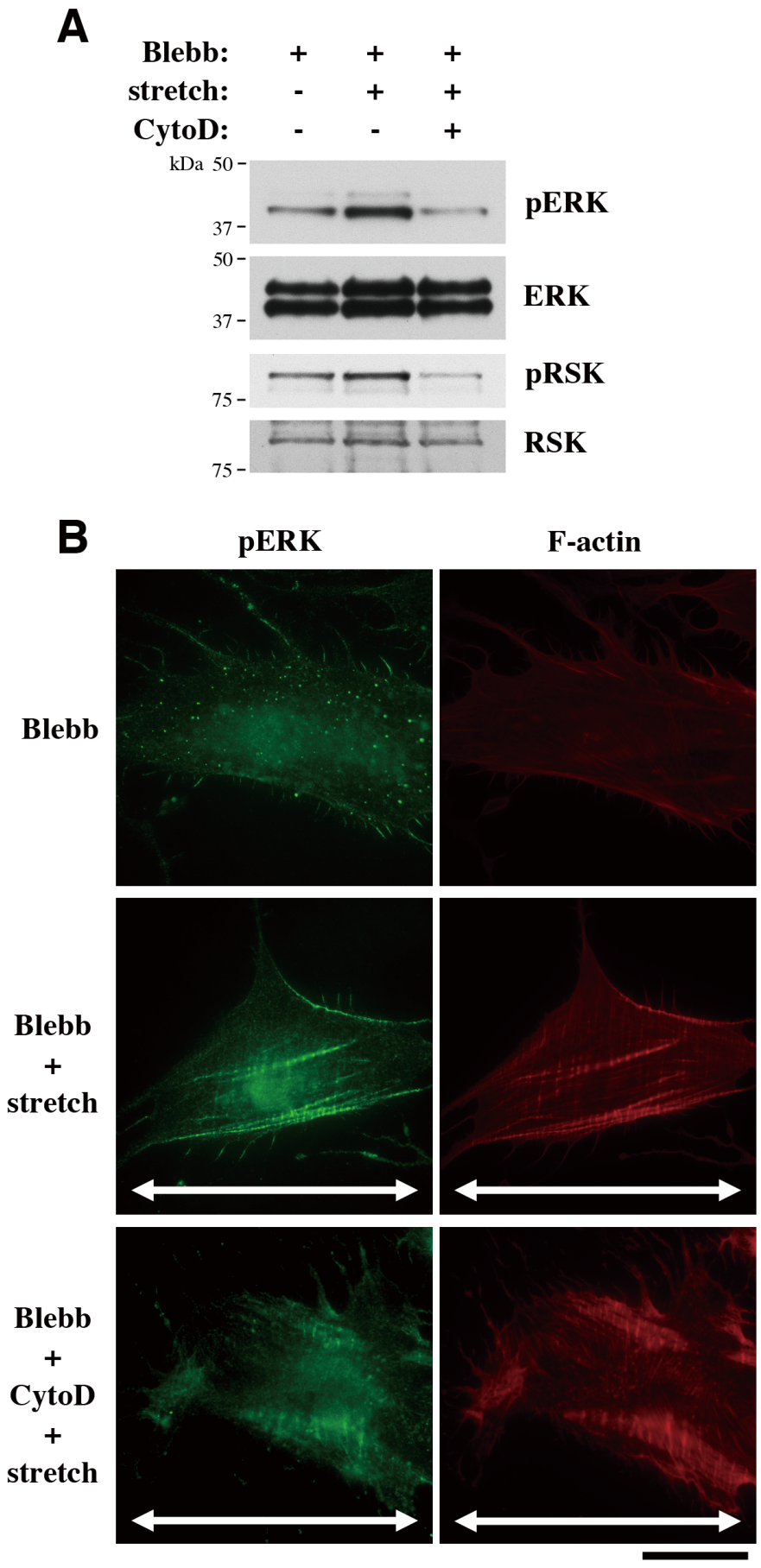
A
Blebb: + + +
stretch: - + +
CytoD: - - +
kDa 50
37
50
37
75
75
pERK
ERK
pRSK
RSK
B
pERK
F-actin
Blebb
Blebb + stretch
Blebb + CytoD + stretch

Fig. S12

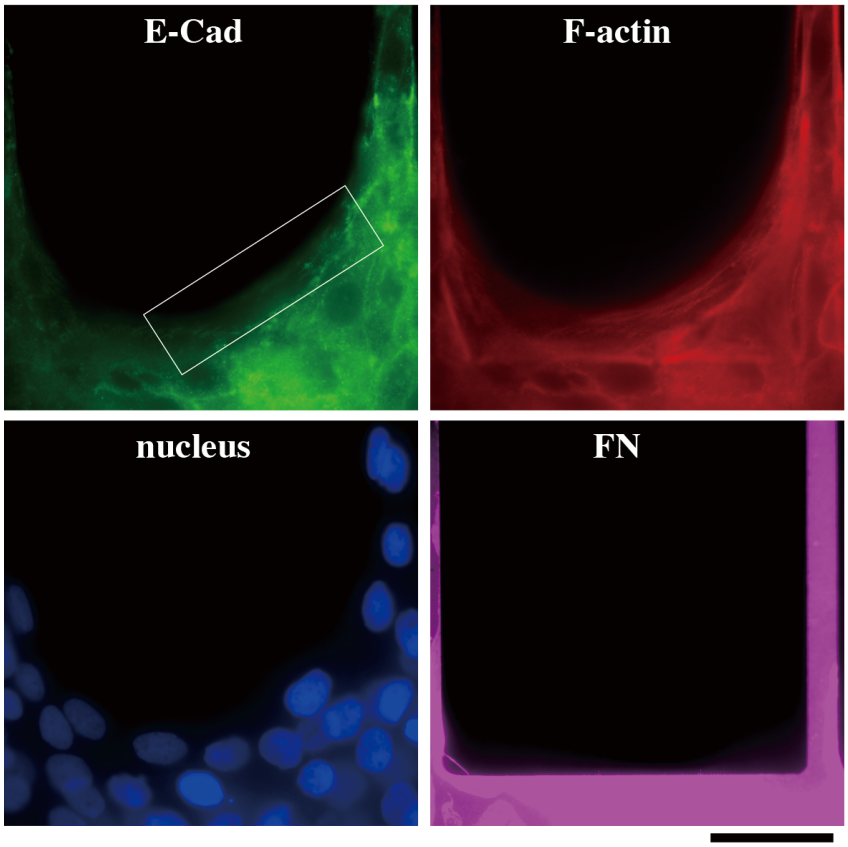

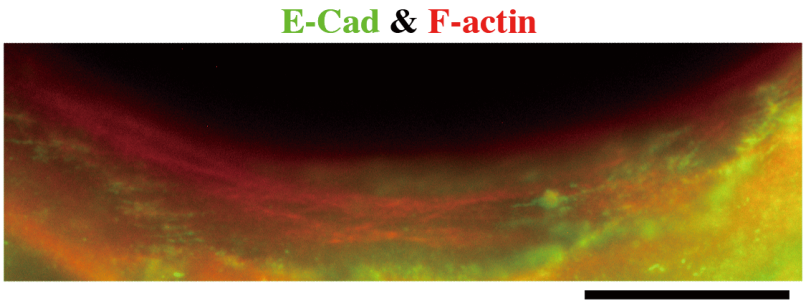

Fig. S13

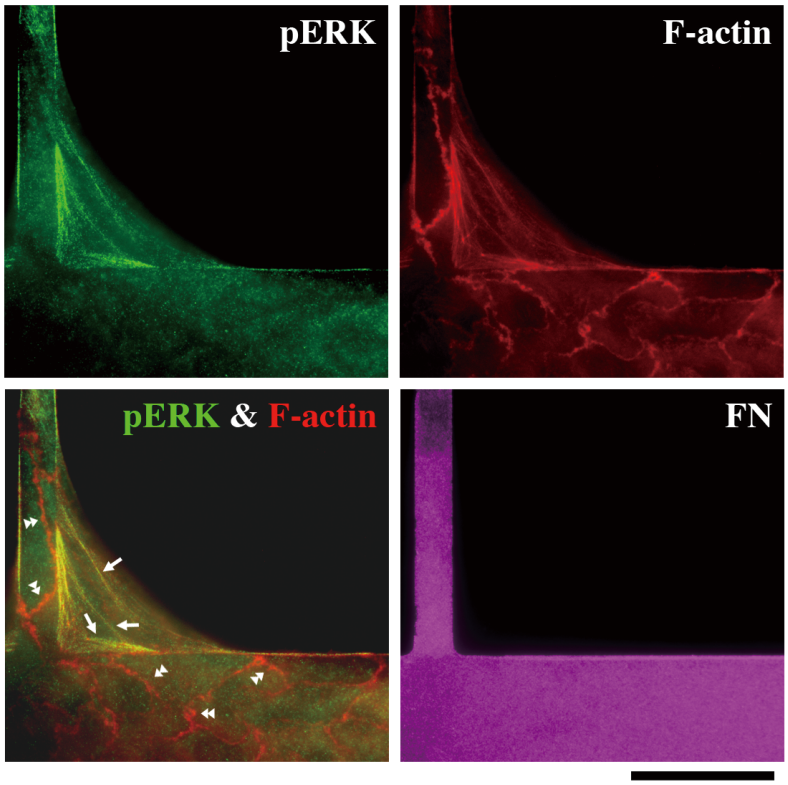

Fig. S14

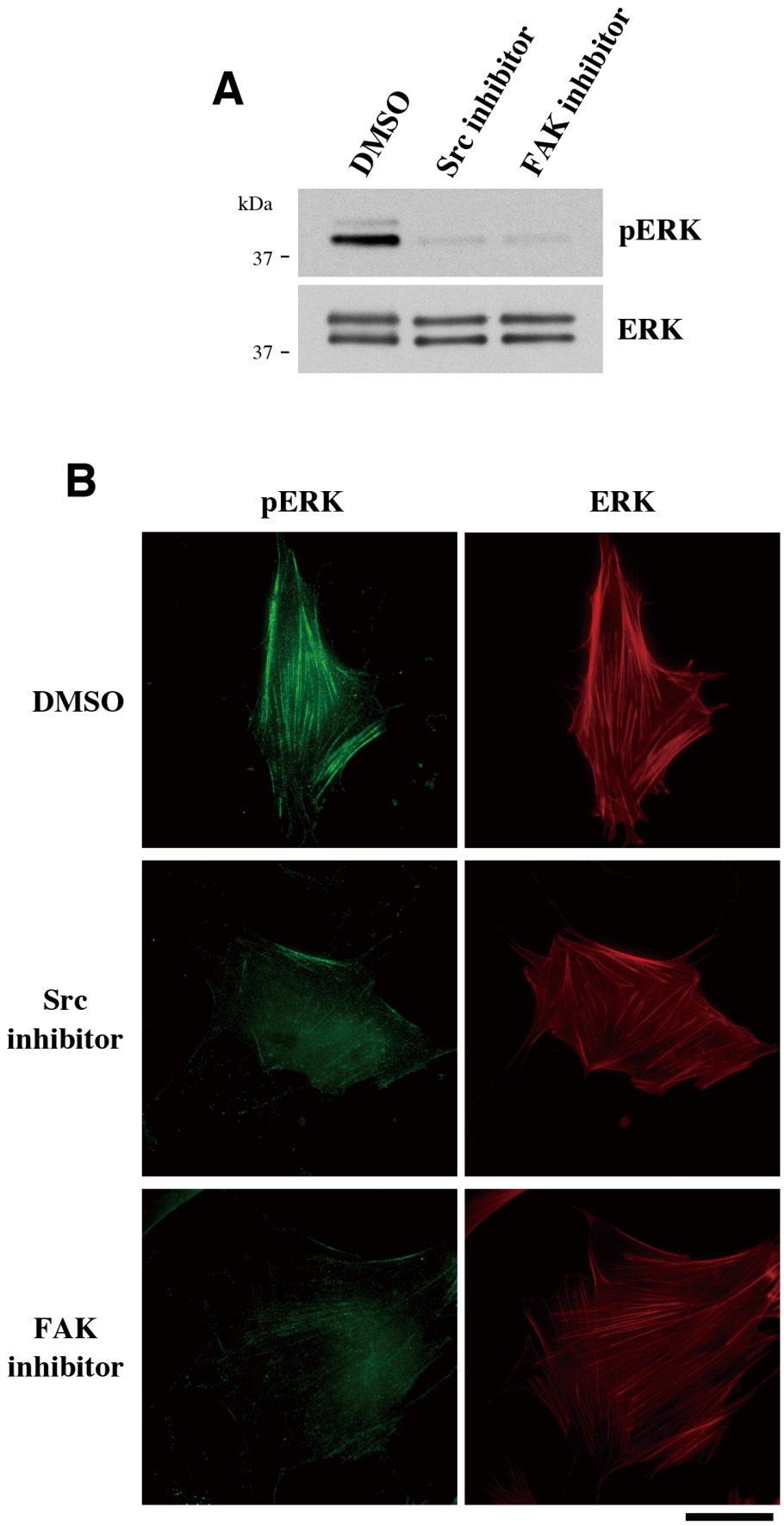
A
DMSO
Src inhibitor
FAK inhibitor
kDa
37
pERK
37
ERK
B
pERK
ERK
DMSO
Src inhibitor
FAK inhibitor

Fig. S15

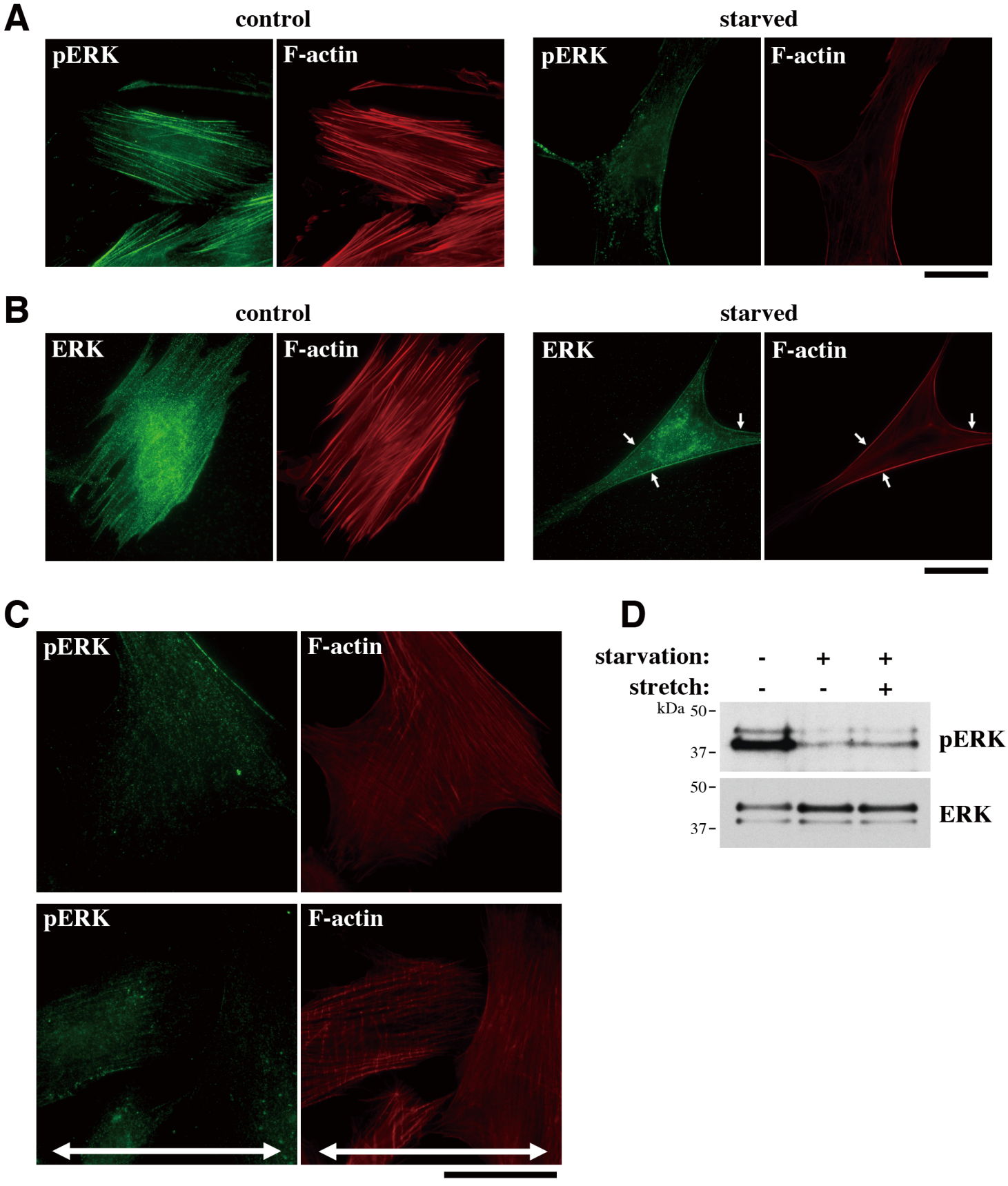
A
control
starved
pERK
F-actin
pERK
F-actin
B
control
starved
ERK
F-actin
ERK
F-actin
C
pERK
F-actin
pERK
F-actin
D
starvation: - + +
stretch: - - +
kDa
50-
37-
pERK
50-
37-
ERK

Fig. S16

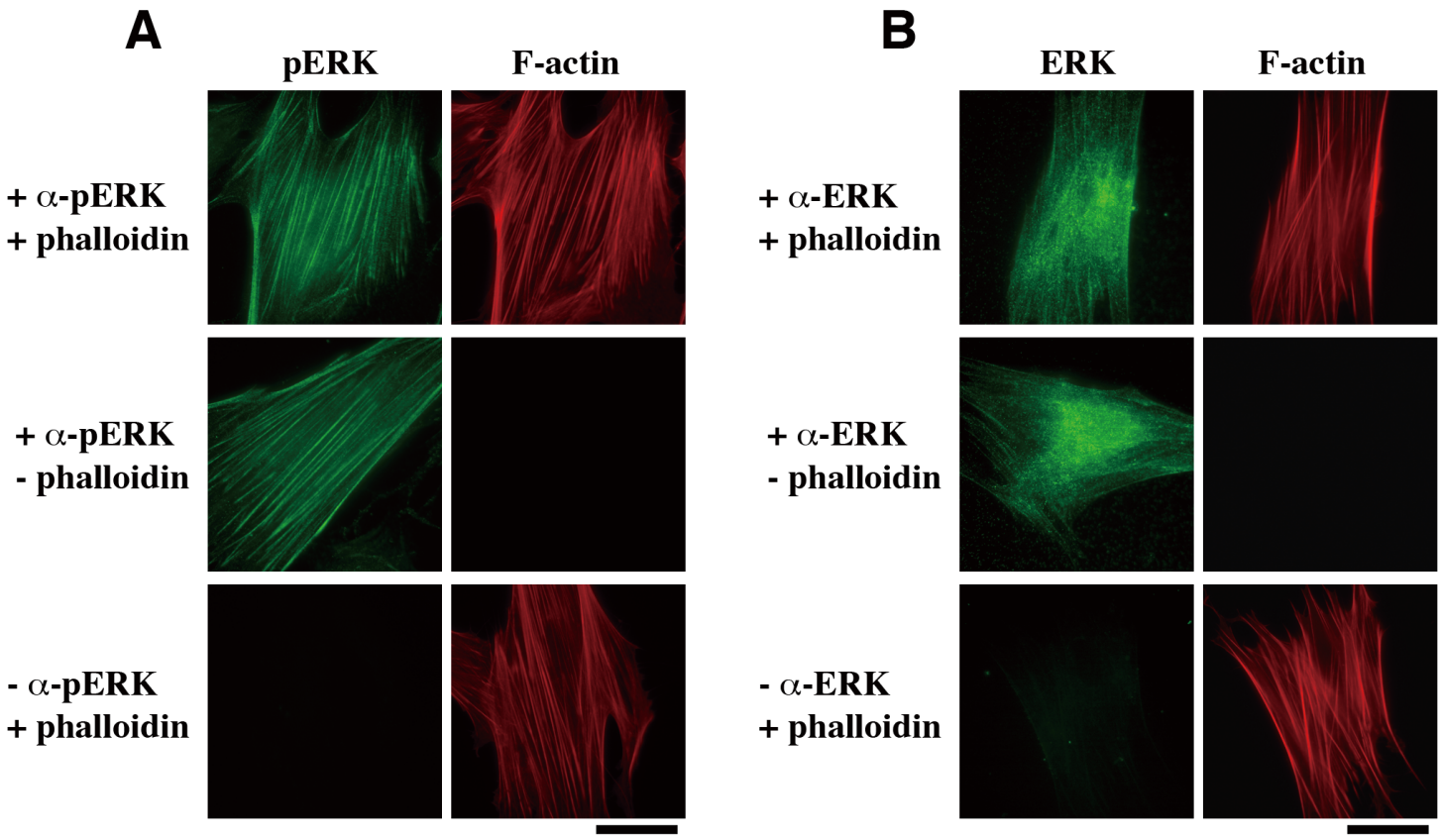
A
pERK
F-actin
+ α-pERK
+ phalloidin
+ α-pERK
- phalloidin
- α-pERK
+ phalloidin
B
ERK
F-actin
+ α-ERK
+ phalloidin
+ α-ERK
- phalloidin
- α-ERK
+ phalloidin

Fig. S17

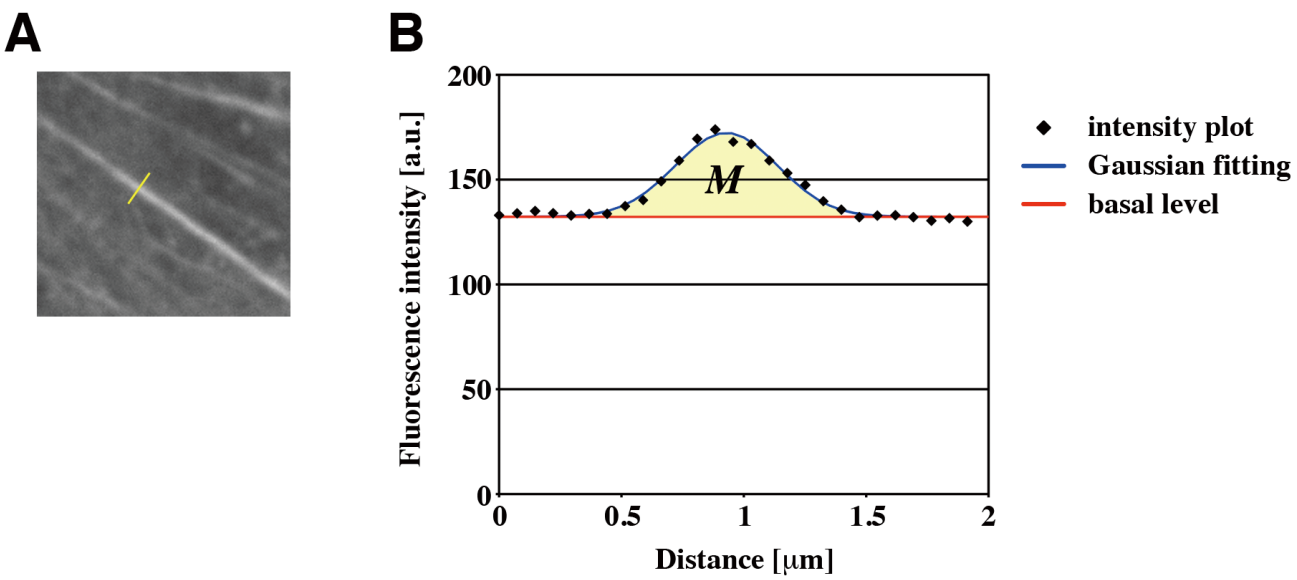
A
B
200
150
100
50
0
0
0.5
1
1.5
2
Fluorescence intensity [a.u.]
Distance [μm]
M
intensity plot
Gaussian fitting
basal level

Fig. S18

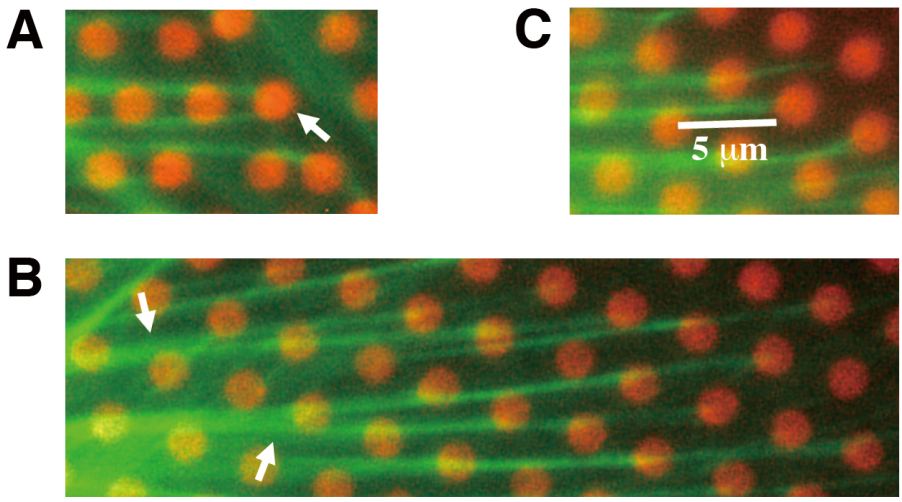

Fig. S19